Nonlinear Valley and Spin Currents from Fermi Pocket Anisotropy in 2D Crystals

Hongyi Yu,[1] Yue Wu,[1] Gui-Bin Liu,[2,1] Xiaodong Xu,[3,4] and Wang Yao[1,*]

[1]*Department of Physics and Center of Theoretical and Computational Physics, The University of Hong Kong, Hong Kong, China*

[2]*School of Physics, Beijing Institute of Technology, Beijing 100081, China*

[3]*Department of Physics, University of Washington, Seattle, Washington 98195, USA*

[4]*Department of Materials Science and Engineering, University of Washington, Seattle, Washington 98195, USA*

(Received 10 June 2014; published 10 October 2014)

The controlled flow of spin and valley pseudospin is key to future electronics exploiting these internal degrees of freedom of carriers. Here, we discover a universal possibility for generating spin and valley currents by electric bias or temperature gradient only, which arises from the anisotropy of Fermi pockets in crystalline solids. We find spin and valley currents to the second order in the electric field as well as their thermoelectric counterparts, i.e., the nonlinear spin and valley Seebeck effects. These second-order nonlinear responses allow two unprecedented possibilities to generate pure spin and valley flows without net charge current: (i) by an ac bias or (ii) by an arbitrary inhomogeneous temperature distribution. As examples, we predict appreciable nonlinear spin and valley currents in two-dimensional (2D) crystals including graphene, monolayer and trilayer transition-metal dichalcogenides, and monolayer gallium selenide. Our finding points to a new route towards electrical and thermal generations of spin and valley currents for spintronic and valleytronic applications based on 2D quantum materials.

DOI: 10.1103/PhysRevLett.113.156603 PACS numbers: 72.25.−b, 72.80.Vp, 73.50.Lw, 85.75.−d

The discovery of atomically thin two-dimensional (2D) crystals has opened up new realms in physics, material science, and engineering [1,2]. The library of 2D crystals now consists of versatile members including graphene and its derivatives, oxides, and transition-metal dichalcogenides (TMDs), offering a variety of appealing material systems, from gapless to direct-gap semiconductors, and from metal to wide-gap insulators [1–3]. A rather common feature of these 2D crystals is the presence of the conduction and valence-band edges at degenerate extrema in momentum space, usually referred to as valleys. The Fermi surface then consists of well-separated pockets at the valleys, which constitute an effective internal degree of freedom of the carrier. The exploitation of the valley pseudospin as well as spin in electronics may significantly extend the device functionalities [4–9]. The recent discoveries of valley physics and spin-valley coupled effects in 2D TMDs have significantly boosted their potential in spintronic and valleytronic applications [10–18].

The generation and control of spin and valley pseudospin currents are at the heart of spintronics and valleytronics [19]. There has been a variety of approaches based on the detail characteristics of different systems, for example, the spin injection or pumping from proximity ferromagnets [20,21] and the various optical injection methods that rely on optical selection rules [22–24]. In time-reversal symmetric systems, the spin Hall effect from spin-orbit coupling [25–28] and the valley Hall effect from inversion symmetry breaking [6,13] have also been explored, with the possibility of implementation in 2D crystals [18,29,30]. The spin or valley Hall current, however, is always accompanied by the longitudinal charge current that is orders of magnitude larger, and such a major cause of dissipation cannot be removed as it has the same linear dependence on the field as the Hall currents.

Here, we discover a new origin of valley and spin currents from the anisotropy of Fermi pockets, a universal feature of crystalline solids. Such valley and spin currents can be generated by the electric bias only and appear in the second order to the electric field. The quadratic dependence on field makes possible current rectification for generation of dc spin and valley currents by ac electric field, with the absence of net charge current. For several exemplary 2D crystals including TMDs monolayers and trilayers, graphene, and GaSe monolayer, we find appreciable nonlinear spin and valley currents in their K, Γ, and Λ valleys. We predict that, at p-n junction in monolayer TMDs [31–33], the nonlinear valley current will result in unique circular polarization pattern of electroluminescence depending on the orientation of the junction relative to the crystalline axis. We also predict the nonlinear valley and spin Seebeck effects, where a temperature gradient can play the same role as the electric field in giving rise to the valley and spin currents. The quadratic dependence of the valley (spin) thermopower on the temperature gradient implies a remarkably simple way to generate pure valley (spin) flow with zero charge current by an inhomogeneous temperature distribution.

We focus here on 2D crystals with mirror symmetry in the out-of-plane (z) direction, where the Bloch states must have their spin either parallel or antiparallel to the z axis. Consider a spin-up Fermi pocket in valley A with dispersion $\mathcal{E}_{A,\uparrow}(\mathbf{q})$, $\mathbf{q}$ being the wave vector measured from A. In an in-plane electric field $\mathbf{E}$, $f(\mathbf{q},\mathbf{E})$ is the steady-state distribution function of carriers. Not concerning the Hall effect, the current is then $\mathbf{j}_{A,\uparrow}(\mathbf{E}) = \int d\mathbf{q} f_{A,\uparrow}(\mathbf{q},\mathbf{E}) \nabla_{\mathbf{q}} \mathcal{E}_{A,\uparrow}(\mathbf{q})$. If $\mathcal{E}_{A,\uparrow}(\mathbf{q}) \neq \mathcal{E}_{A,\uparrow}(-\mathbf{q})$, the current response can also lack the 180° rotational symmetry, i.e., $\mathbf{j}_{A,\uparrow}(\mathbf{E}) \neq -\mathbf{j}_{A,\uparrow}(-\mathbf{E})$. In a time-reversal symmetric system, this current will have a counterpart $\mathbf{j}_{\bar{A},\downarrow}$ from a spin-down pocket at valley $\bar{A}$, the time reversal of A, where $\mathcal{E}_{\bar{A},\downarrow}(\mathbf{q}) = \mathcal{E}_{A,\uparrow}(-\mathbf{q})$. The Boltzmann transport equation under the relaxation time approximation then leads to $f_{\bar{A},\downarrow}(\mathbf{q},\mathbf{E}) = f_{A,\uparrow}(-\mathbf{q},-\mathbf{E})$ (Supplemental Material [34]). These determine $\mathbf{j}_{\bar{A},\downarrow}(\mathbf{E}) = -\mathbf{j}_{A,\uparrow}(-\mathbf{E})$ (Fig. 1). Thus, under the condition of Fermi pocket anisotropy, the currents contributed by the time-reversal pair of Fermi pockets can have a finite difference: $\mathbf{j}_{A,\uparrow}(\mathbf{E}) - \mathbf{j}_{\bar{A},\downarrow}(\mathbf{E}) \neq 0$, which is a valley current as well as a spin current.

We find that such spin and valley currents arise in the second order of the electric field. In an electric field along the x direction, without concerning the Hall effect, the longitudinal and transverse components of $\mathbf{j}_{A,\uparrow}$ can be expanded as (see the Supplemental Material [34])

$$j^x_{A,\uparrow}(\mathbf{E}) = \sigma^{xx}_{A,\uparrow} E + \sigma^{xxx}_{A,\uparrow} E^2 + O(E^3),$$
$$j^y_{A,\uparrow}(\mathbf{E}) = \sigma^{yxx}_{A,\uparrow} E^2 + O(E^3). \tag{1}$$

As $\mathbf{j}_{\bar{A},\downarrow}(-\mathbf{E}) = -\mathbf{j}_{A,\uparrow}(\mathbf{E})$, we have $\sigma^{xxx}_{A,\uparrow} = -\sigma^{xxx}_{\bar{A},\downarrow}$, $\sigma^{yxx}_{A,\uparrow} = -\sigma^{yxx}_{\bar{A},\downarrow}$, while $\sigma^{xx}_{A,\uparrow} = \sigma^{xx}_{\bar{A},\downarrow}$. The charge current is $\mathbf{j}_{A,\uparrow}(\mathbf{E}) + \mathbf{j}_{\bar{A},\downarrow}(\mathbf{E}) = 2\hat{\mathbf{x}}\sigma^{xx}_{A,\uparrow} E + O(E^3)$, an odd function of the electric field, while the valley (spin) current is $\mathbf{j}_{A,\uparrow}(\mathbf{E}) - \mathbf{j}_{\bar{A},\downarrow}(\mathbf{E}) = 2(\hat{\mathbf{x}}\sigma^{xxx}_{A,\uparrow} + \hat{\mathbf{y}}\sigma^{yxx}_{A,\uparrow})E^2$, an even function of the field. On application of an ac electric field $E_x = E\cos\omega t$, the dc charge current is zero, and the valley (spin) current becomes

$$\mathbf{j}_{A,\uparrow} - \mathbf{j}_{\bar{A},\downarrow} = (\hat{\mathbf{x}}\sigma^{xxx}_{A,\uparrow} + \hat{\mathbf{y}}\sigma^{yxx}_{A,\uparrow})E^2(1 + \cos 2\omega t). \tag{2}$$

In addition to a second harmonic term, the valley (spin) current has a dc component. We note that Eq. (2) implicitly assumes ω^{-1} being larger than the momentum relaxation time τ, as it is based on the steady state response in Eq. (1). From the symmetry alone, we expect this rectification effect can exist even beyond the regime of $\omega\tau < 1$.

Monolayer (ML) group-VIB TMDs provide an excellent system to illustrate the different scenarios of the nonlinear spin and valley currents (Fig. 2). The top valence band in ML TMDs has local maxima at both Γ and K ($\bar{K}$) points. The lowest conduction band has two types of local minima: the K ($\bar{K}$) point and the low-symmetry Λ ($\bar{\Lambda}$) points between K ($\bar{K}$) and Γ.

For the Fermi pockets at K ($\bar{K}$), the anisotropy is the trigonal warping [44,45], which breaks the 180° rotational symmetry of the pockets. Both the conduction and the valence bands are spin split in the K valleys [13,46]. If the Fermi energy is between the split bands, we only have a spin-up (-down) Fermi pocket at K ($\bar{K}$). Valley current is then the same as spin current. If the field is applied along a zigzag direction, the valley (spin) current is either parallel or antiparallel to the field because of the reflection symmetry of the Fermi pocket [Fig. 2(a)]. For electric field in the armchair direction, we find the valley (spin) current perpendicular to the field [Figs. 2(d) and 2(e)].

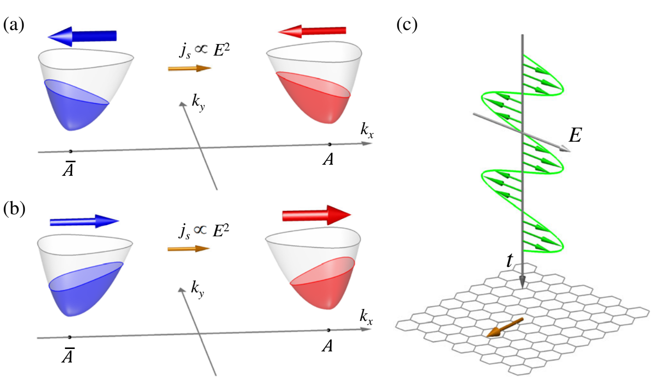

FIG. 1 (color online). (a), (b) Carrier distributions of a spin-up Fermi pocket at valley A and a spin-down pocket at valley $\bar{A}$, in an electric field along $+x$ (a) or $-x$ (b) direction. The anisotropy of the Fermi pocket results in a difference in the currents from A and $\bar{A}$, giving rise to a valley (spin) current quadratic in the field. The horizontal red (blue) arrows correspond to the current from the Fermi pocket A ($\bar{A}$), with the arrow thickness denoting the magnitude. (c) Such quadratic dependence in the field makes possible the generation of dc valley and spin currents by ac electric field, in the absence of net charge current.

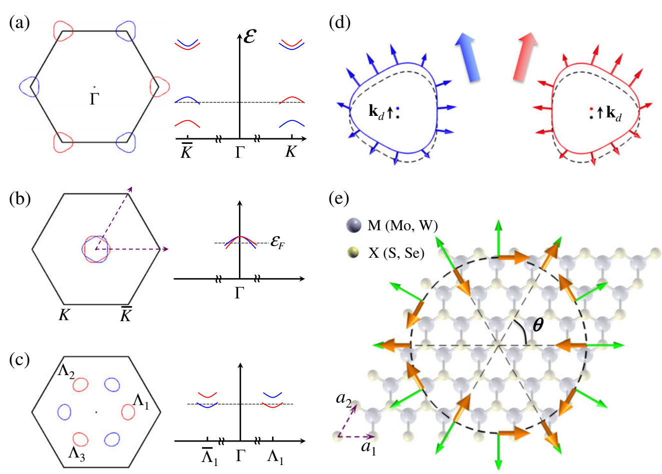

FIG. 2 (color online). (a) Hole pockets at K valleys, (b) at Γ point, and (c) electron pockets at Λ valleys in monolayer TMDs. Red (blue) denotes spin up (down). (d) Displacement of K pockets by an electric field in the armchair direction, where the thick red (blue) arrow corresponds to the current from the Fermi pocket K ($\bar{K}$). The valley (spin) current flows perpendicular to the field. The thin red (blue) arrows illustrate the group velocity on the displaced K ($\bar{K}$) valley Fermi surface. (e) Dependence of the spin valley current direction (orange arrow) on the relative angle θ between the field (green arrow) and the crystalline axis.

TABLE I. Spin current (j_s) and valley current (j_v) in several hexagonal 2D crystals. The direction angles of the current ($\theta_{s/v}$) and the field (θ) are both defined with respect to a zigzag axis.

	Monolayer MoS_2				Trilayer MoS_2		GaSe	Graphene
	K, h	K, e[a]	Λ, e	Γ, h	Λ, e[a]	Γ, h	Λ, h[a]	K, e (h)
j_s $(12\pi/\hbar)$	$\beta\mathcal{E}_F k_d^2$	$\beta\Delta k_d^2$	$3\beta\mathcal{E}_F k_d^2$	$\beta\mathcal{E}_F k_d^2$	$3\beta\Delta k_d^2$	$\beta\mathcal{E}_F k_d^2$	$3\beta\Delta k_d^2$	0
j_v $(12\pi/\hbar)$	$\beta\mathcal{E}_F k_d^2$	$\beta(2\mathcal{E}_F-\Delta)k_d^2$	[b]		[b]		[b]	$\beta\mathcal{E}_F k_d^2$
β (Å)	−0.94	−0.49	0.33	−0.12	0.09	−0.01	−1.62	−0.36
$\theta_{v(s)}$	$\pi-2\theta$	$\pi-2\theta$	-2θ	$\pi-2\theta$	-2θ	$\pi-2\theta$	$\pi-2\theta$	$\pi-2\theta$

[a]For these cases we assume $\mathcal{E}_F$ is larger than the small spin splitting Δ so that both spin bands are occupied at each valley.
[b]Valley current is finite but lacks a unique definition.

The trigonal warping also exists for the hole pocket at Γ point. By the time-reversal symmetry, the warping is opposite for the spin-up and spin-down pockets [Fig. 2(b)], giving rise to a nonlinear spin current. At the six low-symmetry Λ valleys in the conduction band [Fig. 2(c)], the anisotropy leads to valley-dependent current response to electric field as well as an overall spin current contributed by all Λ and $\bar{\Lambda}$ pockets. The direction of spin current from Γ or Λ pockets as a function of field orientation is also similar to that of the K pockets [Fig. 2(e) and Table I].

The magnitude of the nonlinear spin and valley currents depends on the dispersion of the Fermi pockets and the distribution function in electric field. For the latter, we adopt the commonly used relaxation time approximation. Consider, for example, the K valleys in ML TMDs, the dispersion of either the electron or the hole near the Fermi surface can be well fit by [44,45]

$$\mathcal{E}_K(\mathbf{q}) = \frac{\hbar^2 q^2}{2m^*}(1+\beta q\cos 3\theta_q), \tag{3}$$

where $\mathbf{q} \equiv (q\cos\theta_q, q\sin\theta_q)$, and β has weak dependence on the Fermi energy (see the Supplemental Material [34]). Neglecting the spin and valley relaxations, the spin and valley currents are (cf. Supplemental Material [34])

$$\mathbf{j}_s = \mathbf{j}_v = \frac{12\pi}{\hbar}\mathcal{E}_F\beta|\mathbf{k}_d|^2(\cos 2\theta, -\sin 2\theta) + O(|\mathbf{k}_d|^4), \tag{4}$$

where $\mathcal{E}_F$ is the Fermi energy measured from the band edge, $\mathbf{k}_d = e\tau\mathbf{E}/\hbar$, $\mathbf{E} \equiv (E\cos\theta, E\sin\theta)$, and τ is the momentum relaxation time. Clearly, the effect favors large mobility. Taking the mobility value ~ 1000 $cm^2\,V^{-1}\,s^{-1}$ measured at low temperature [47] (or ~ 200 $cm^2\,V^{-1}\,s^{-1}$ at room temperature [48,49]), we estimate the nonlinear valley current starts to exceed the observed sizable valley Hall current [13,18] at an electric field of ~ 10 $mV\,\mu m^{-1}$ (~ 0.25 $V\,\mu m^{-1}$) (Supplemental Material [34]).

The charge current normalized by e is $\mathbf{j}_c = [(4\pi)/\hbar]\mathcal{E}_F\mathbf{k}_d + O(|\mathbf{k}_d|^3)$. The ratio of the spin and valley currents to the charge current is

$$j_s/j_c = j_v/j_c = 3\beta e\tau E/\hbar. \tag{5}$$

Interestingly, this ratio is independent of $\mathcal{E}_F$. We note that Eq. (4) is for the situation where $\mathcal{E}_F$ lies between the spin split bands [cf. Fig. 2(a)]. This is always the case for p-doped ML TMDs because of the giant spin splitting. For n doping, if the higher spin split band is also occupied, it will have a contribution also given by Eq. (4), but with $\mathbf{j}_s = -\mathbf{j}_v$ (Supplemental Material [34]). Equation (4) still holds for the valley current, but the overall spin current can then differ from the valley current, as listed in Table I.

For the Γ hole pockets in ML TMDs, the dispersion can be described by Eq. (3) as well, which leads to the spin current given by Eq. (4). The Λ electron pockets in ML TMDs have a more complicated dispersion. Nevertheless, the overall spin current from all Λ and $\bar{\Lambda}$ pockets is still given by Eq. (4) (Supplemental Material [34]). The degrees of the anisotropy β for the K, Γ, and Λ pockets obtained by fitting the *ab initio* bands are listed in Table I for ML MoS_2; β in MLs $MoSe_2$, WS_2, and WSe_2 are found to have comparable magnitudes (Supplemental Material [34]). In ML TMDs, the Γ and Λ pockets only appear at very large p and n doping, respectively. In trilayer TMDs, Γ and Λ can be the valence and conduction band edges, respectively, and we find nonlinear spin and valley currents given by Eq. (4) as well [34]. Table I also lists the nonlinear spin current in p-doped monolayer GaSe, where the Fermi pockets are at the Λ points [50], and the result is similar to the TMDs.

Graphene is an example with two representative differences from the scenarios discussed above. First, the bands are spin degenerate so that spin current must vanish. Second, the band dispersion is linear to the leading order. The conduction and valence bands dispersion at the K and $\bar{K}$ valleys are described by $\mathcal{E}_K(\mathbf{q}) = \pm\hbar v_F q(1+\beta q\cos 3\theta_q + O(q^2))$. Such dispersion can lead to valley-dependent tunneling at potential barriers [51,52]. Interestingly, we find that, in graphene, the nonlinear valley current is still given by Eq. (4), and the ratio of the valley current to charge current is given by Eq. (5) (Supplemental Material [34]).

Equations (4) and (5) are derived for the low-temperature regime $\mathcal{E}_F \gg k_B T$. Beyond this regime, the spin and valley currents will depend on temperature. Nevertheless, Eq. (5) for the valley to charge current ratio will still hold, as this ratio is nearly independent of $\mathcal{E}_F$ and, hence, the filling of the states in equilibrium (Supplemental Material [34]).

The emerging monolayer and multilayer TMD p-n junction devices [31–33] provide an ideal laboratory for the exploration of nonlinear valley and spin currents. Under forward bias, electrons (holes) from the K valleys in the n (p) region will reach the junction and produce electroluminescence (EL) through recombination. If the junction is along the armchair direction, the valley (spin) current is collinear to the charge current, and carriers accumulated in the junction region are valley polarized. With the valley-dependent optical selection rule [7,13–17], we expect that the EL will have an overall circular polarization [Fig. 3(a)]. Given a reasonable forward bias $E \sim 10\ \mathrm{V}\,\mu\mathrm{m}^{-1}$, the EL polarization is estimated to be ~20% (Supplemental Material [34]), which changes sign when the p-n junction flips [Fig. 3(a)]. This nonlocal valley transport effect is in qualitative agreement with the polarized EL reported very recently in thin flake WSe_2 p-n junctions [53].

Our theory also predicts a unique spatial pattern of EL polarization when the junction is not along the armchair direction, which distinguishes it from other possible mechanisms for the polarized EL [13,53]. Consider a p-n junction along the zigzag direction, where the valley (spin) current is perpendicular to the charge current, and carriers will accumulate with opposite valley polarizations at the two sides where the EL will then have opposite circular polarization. This spatial dependence clearly distinguishes the nonlocal valley transport here from the effect of local change in the population of recombining electrons and holes by the electric field at depletion region proposed in Ref. [53]. The effect is also distinct from the valley Hall current [6,13,18]. When p-n junction flips sign, the EL polarization on the two sides will change sign if it arises from the valley Hall effect but will remain unchanged if it is from the nonlinear valley current [Fig. 3(b)].

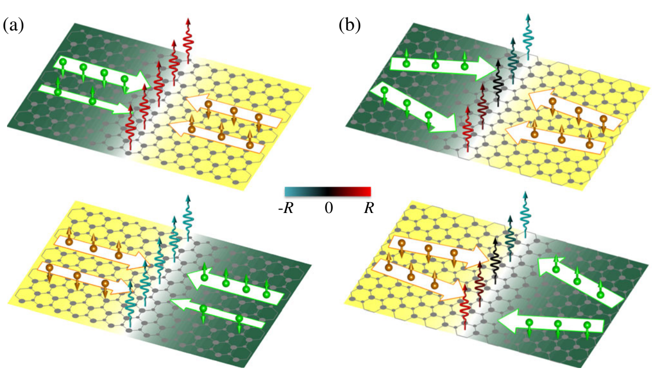

FIG. 3 (color online). (a) Polarized EL from p-n junction along armchair direction. The EL has an overall circular polarization $R \sim j_v/j_c$. Green (yellow) color denotes the hole (electron) doped region, and red (blue) color denotes the $\sigma-$ ($\sigma+$) circular polarization. The hole has larger anisotropy and, hence, larger nonlinear valley current, which determines the EL polarization. (b) Spatial pattern of EL polarization from p-n junction along the zigzag direction.

Similar to that in an electric field, we find the second-order nonlinear response to a temperature gradient ∇T is a pure valley (spin) current, while the linear response is a charge current (Supplemental Material [34]). Taking the K pockets in ML TMDs, for example, the direction of nonlinear valley current is also given by Fig. 2(e), where θ now represents the relative angle between the direction of ∇T (green arrows) and a zigzag axis. If $T/|\nabla T|$ is much larger than the mean free path, we find the ratio between the valley and charge currents (Supplemental Material [34])

$$j_v/j_c = \frac{6}{\hbar}\alpha\beta k_B|\nabla T|\tau, \tag{6}$$

where the dimensionless coefficient α is a function of $\mathcal{E}_F/k_BT$ only, as shown in Fig. 4(a).

For $\mathcal{E}_F \gg k_BT$, we find $\alpha \cong \mathcal{E}_F/k_BT$, and the valley current is given by

$$\mathbf{j}_v(\nabla T) = \frac{8\pi^3}{\hbar^3}\mathcal{E}_F\beta k_B^2|\nabla T|^2\tau^2(\cos 2\theta, -\sin 2\theta). \tag{7}$$

Interestingly, comparing this with Eq. (4), we find

$$\left(\frac{1}{k_B|\nabla T|}\right)^2 \mathbf{j}_v(\nabla T) = \frac{2\pi^2}{3}\left(\frac{1}{eE}\right)^2 \mathbf{j}_v(\mathbf{E}), \tag{8}$$

which holds true for the other cases of nonlinear spin and valley currents discussed in Table I.

The quadratic dependence of valley and spin currents on the temperature gradient makes possible the generation of pure valley and spin flows. Consider an arbitrary inhomogeneous temperature distribution where the temperatures at the two ends of the device are equal; the charge current is then zero, but the valley (spin) current is finite [Fig. 4(b)]. This is an unprecedented simple way for generating pure valley and spin flows.

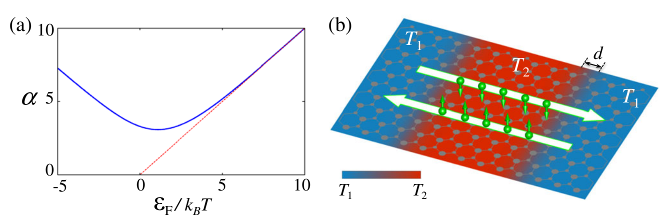

FIG. 4 (color online). (a) The dimensionless coefficient α that measures the ratio between the valley (spin) current and the charge current by a temperature gradient [see Eq. (6)]. (b) Spin and valley currents can be generated by an arbitrary inhomogeneous temperature distribution. The charge current vanishes as long as the temperatures at the two ends of the device equal.

The authors thank Jiang Xiao for helpful discussions. This work is mainly supported by the Croucher Foundation under the Croucher Innovation Award, the Research Grant Council (HKU17305914P, HKU9/CRF/13G) and the University Grant Committee (AoE/P-04/08) of Hong Kong SAR. G.-B. L. is also supported by the NSFC (11304014), the 973 Program (2013CB934500) of China, and BIT Basic Research Funds (20131842001, 20121842003). X. X. is supported by the U.S. DOE, BES, Materials Sciences and Engineering Division (DE-SC0008145), the NSF (DMR-1150719), and the Cottrell Scholar Award.

*wangyao@hku.hk

[1] A. K. Geim and I. V. Grigorieva, Nature (London) **499**, 419 (2013).
[2] K. S. Novoselov, D. Jiang, F. Schedin, T. J. Booth, V. V. Khotkevich, S. V. Morozov, and A. K. Geim, Proc. Natl. Acad. Sci. U.S.A. **102**, 10451 (2005).
[3] L. Li, Y. Yu, G. J. Ye, Q. Ge, X. Ou, H. Wu, D. Feng, X. H. Chen, and Y. Zhang, Nat. Nanotechnol. **9**, 372 (2014).
[4] O. Gunawan, B. Habib, E. P. De Poortere, and M. Shayegan, Phys. Rev. B **74**, 155436 (2006).
[5] A. Rycerz, J. Tworzydło, and C. W. J. Beenakker, Nat. Phys. **3**, 172 (2007).
[6] D. Xiao, W. Yao, and Q. Niu, Phys. Rev. Lett. **99**, 236809 (2007).
[7] W. Yao, D. Xiao, and Q. Niu, Phys. Rev. B **77**, 235406 (2008).
[8] Z. Zhu, A. Collaudin, B. Fauqué, W. Kang, and K. Behnia, Nat. Phys. **8**, 89 (2012).
[9] Y. Jiang, T. Low, K. Chang, M. I. Katsnelson, and F. Guinea, Phys. Rev. Lett. **110**, 046601 (2013).
[10] Z. Gong, G.-B. Liu, H. Yu, D. Xiao, X. Cui, X. Xu, and W. Yao, Nat. Commun. **4**, 2053 (2013).
[11] X. Xu, W. Yao, D. Xiao, and T. F. Heinz, Nat. Phys. **10**, 343 (2014).
[12] H. Yuan *et al.*, Nat. Phys. **9**, 563 (2013).
[13] D. Xiao, G.-B. Liu, W. Feng, X. Xu, and W. Yao, Phys. Rev. Lett. **108**, 196802 (2012).
[14] H. Zeng, J. Dai, W. Yao, D. Xiao, and X. Cui, Nat. Nanotechnol. **7**, 490 (2012).
[15] K. F. Mak, K. He, J. Shan, and T. F. Heinz, Nat. Nanotechnol. **7**, 494 (2012).
[16] T. Cao *et al.*, Nat. Commun. **3**, 887 (2012).
[17] A. M. Jones *et al.*, Nat. Nanotechnol. **8**, 634 (2013).
[18] K. F. Mak, K. L. McGill, J. Park, and P. L. McEuen, Science **344**, 1489 (2014).
[19] F. Pulizzi, Nat. Mater. **11**, 367 (2012).
[20] J. Xiao, G. E. W. Bauer, K.-c. Uchida, E. Saitoh, and S. Maekawa, Phys. Rev. B **81**, 214418 (2010).
[21] N. Tombros, C. Jozsa, M. Popinciuc, H. T. Jonkman, and B. J. v. Wees, Nature (London) **448**, 571 (2007).
[22] S. D. Ganichev, E. L. Ivchenko, V. V. Bel'kov, S. A. Tarasenko, M. Sollinger, D. Weiss, W. Wegscheider, and W. Prettl, Nature (London) **417**, 153 (2002).
[23] M. J. Stevens, A. L. Smirl, R. D. R. Bhat, A. Najmaie, J. E. Sipe, and H. M. van Driel, Phys. Rev. Lett. **90**, 136603 (2003).
[24] H. Yuan *et al.*, Nat. Nanotechnol. **9**, 851 (2014).
[25] S. Murakami, N. Nagaosa, and S.-C. Zhang, Science **301**, 1348 (2003).
[26] J. Sinova, D. Culcer, Q. Niu, N. A. Sinitsyn, T. Jungwirth, and A. H. MacDonald, Phys. Rev. Lett. **92**, 126603 (2004).
[27] Y. K. Kato, R. C. Myers, A. C. Gossard, and D. D. Awschalom, Science **306**, 1910 (2004).
[28] T. Jungwirth, J. Wunderlich, and K. Olejník, Nat. Mater. **11**, 382 (2012).
[29] D. A. Abanin *et al.*, Science **332**, 328 (2011).
[30] J. Balakrishnan, G. K. W. Koon, M. Jaiswal, A. H. Castro Neto, and B. Özyilmaz, Nat. Phys. **9**, 284 (2013).
[31] A. Pospischil, M. M. Furchi, and T. Mueller, Nat. Nanotechnol. **9**, 257 (2014).
[32] B. W. H. Baugher, H. O. H. Churchill, Y. Yang, and P. Jarillo-Herrero, Nat. Nanotechnol. **9**, 262 (2014).
[33] J. S. Ross *et al.*, Nat. Nanotechnol. **9**, 268 (2014).
[34] See the Supplemental Material at http://link.aps.org/supplemental/10.1103/PhysRevLett.113.156603, which includes Refs. [35–43], for details on the nonlinear valley and spin currents in the relaxation time approximation, comparison to valley Hall current in monolayer TMDs, and *ab initio* calculations.
[35] B. M. Askerov, *Electron Transport Phenomena in Semiconductors* (World Scientific, Singapore, 1994), Vol. 394.
[36] M. Cutler and N. F. Mott, Phys. Rev. **181**, 1336 (1969).
[37] B. Radisavljevic and A. Kis, Nat. Mater. **12**, 815 (2013).
[38] K. Kaasbjerg, K. S. Thygesen, and K. W. Jacobsen, Phys. Rev. B **85**, 115317 (2012).
[39] G. Kresse and J. Furthmüller, Phys. Rev. B **54**, 11169 (1996).
[40] J. P. Perdew, K. Burke, and M. Ernzerhof, Phys. Rev. Lett. **77**, 3865 (1996).
[41] S. Grimme, J. Comput. Chem. **27**, 1787 (2006).
[42] W. Han, J.-R. Chen, D. Wang, K. M. McCreary, H. Wen, A. G. Swartz, J. Shi, and R. K. Kawakami, Nano Lett. **12**, 3443 (2012).
[43] K. M. Borysenko, J. T. Mullen, E. A. Barry, S. Paul, Y. G. Semenov, J. M. Zavada, M. B. Nardelli, and K. W. Kim, Phys. Rev. B **81**, 121412 (2010).
[44] G.-B. Liu, W.-Y. Shan, Y. Yao, W. Yao, and D. Xiao, Phys. Rev. B **88**, 085433 (2013).
[45] A. Kormányos, V. Zólyomi, N. D. Drummond, P. Rakyta, G. Burkard, and V. I. Fal'ko, Phys. Rev. B **88**, 045416 (2013).
[46] Z. Y. Zhu, Y. C. Cheng, and U. Schwingenschlögl, Phys. Rev. B **84**, 153402 (2011).
[47] B. W. H. Baugher, H. O. H. Churchill, Y. Yang, and P. Jarillo-Herrero, Nano Lett. **13**, 4212 (2013).
[48] H. Fang, S. Chuang, T. C. Chang, K. Takei, T. Takahashi, and A. Javey, Nano Lett. **12**, 3788 (2012).
[49] W. Liu, J. Kang, D. Sarkar, Y. Khatami, D. Jena, and K. Banerjee, Nano Lett. **13**, 1983 (2013).
[50] V. Zólyomi, N. D. Drummond, and V. I. Fal'ko, Phys. Rev. B **87**, 195403 (2013).
[51] J. M. Pereira, Jr., F. M. Peeters, R. N. Costa Filho, and G. A. Farias, J. Phys. Condens. Matter **21**, 045301 (2009).
[52] J. L. Garcia-Pomar, A. Cortijo, and M. Nieto-Vesperinas, Phys. Rev. Lett. **100**, 236801 (2008).
[53] Y. J. Zhang, T. Oka, R. Suzuki, J. T. Ye, and Y. Iwasa, Science **344**, 725 (2014).